An X-ray Study of Hydrogen Induced Phenomenon of Carbon Steel and Austenitic Stainless Steel

Kazuyoshi KAMACHI*

(Received July 15, 1976)

Abstract

Charged hydrogen in metals and alloys cause various effects on their mechanical properties such as embrittlement, delayed fracture and induction of phase transformation.

An X-ray observation of these effects are carried out in carbon steel and austenitic stainless steels.

I. Introduction

There are two sorts of theoretical streams in considering the effects of hydrogen on mechanical properties of metals and alloys. One of it is fracture problem that pre-existted cracks or voids are enlarged by hydrogen gas pressure, assisted by external or internal stresses. Another one is the embrittlement that is reduction of ductility apart from crack propagation.

Several theories have been suggested about the mechanism of hydrogen embrittlement. For example; Zapffe's theory[1] of gas pressure in rift net work of crystalline aggregate; Kazinczy's theory[2] of hydrogen gas in Griffith cracks; and Petch's theory[3] of enlowering of surface energy by hydrogen adsorption, are belonging to the former stream.

Morlet, Johnson and Troiano's work[4] lead to the conclusion that hydrogen embrittlement depend on hydrogen in solid solution in the crystal lattice as well as that entrapping in void under their equilibrium.

Later stream of reduction of ductility is based on the interaction of hydrogen with lattice defects that are dislocation and vacancies.

The interaction of hydrogen and dislocation are discussed by several researchers using the measurement of damping capacity.

In X-ray field, one of the most interesting experiments was reported[5] by Professor Plusquellec, Azou and Bastien that the Laue photograph taken from hydrogenated specimen of armco iron shows blured spots of (112) and (123) reflection, whereas another spots are remainded sharp.

This fact is explained by hydrogen atom trapped by Cottrell atmosphere on the slip plane of iron crystal and it accounted for the hydrogen embrittlement.

Recently, the bonding nature of hydrogen with metal atom and the electronic structure of these interaction are discussed by Professor E. Fujita[6].

Carbon steel is a widely known material as concerned as hydrogen embrittlement

* Department of Industrial Mechanical Fngineering

and delayed fracture from its wide using range, but hydrogen in austenitic stainless steel plays an important role in their corrosive nature as well as embrittlement. The most interesting phenomenon is phase transformation, hydride formation and surface cracking.

These hydrogen induced phenomenon in the two sorts of materials have been investigated mainly using X-ray diffraction technique.

II. Experimental Procedure

(II–1) Carbon Steel and Iron Single Crystal.

Hydrogen was charged in carbon steel (0.16% carbon contented commersial use plate) and iron single crystal after fully annealed. The X-ray diffraction patterns were compared with before and after the charging.

The X-ray diffraction method by diffractmeter was used in measurements of the broadening of diffraction patterns by hydrogen charge. The microfocus X-ray apparatus was used to take pseudo-Kossel patterns of single crystals.

Hydrogen was charged cathodically into the specimens at a current density of 0.1 Amp./cm^2 in an electrolyte cell with a platinum wire anode, and 0.1 N H_2SO_4 electrolytical aqua-solution added with As_2O_3.

X-ray examination was made on heat treated specimen in hydrogen gas atmosphere also, to compare the effect of absorbed hydrogen from cathodically charged condition. The same sorts of observation about diffused-in hydrogen, from acid dipping or H_2S solution immersion were made.

(II–2) Austenitic Stainless Steel

The SUS 304, 316 and 310s type stainless steels were used of which chemical components are shown in Table 1.

Hydrogen charged conditions are the same with the case of cabon steel. To see structure changes in austenite of stainless steels, specimens for transmission electron microscopy were thinned in an electrolyte with H_3PO_4 and Cr_2O_3, and an electron microscope was operated at 200 KV.

Table 1 Chemical Composition (wt %)

Material	C	Si	Mn	P	S	Ni	Cr	Mo
SUS 304	0.06	0.55	1.09	0.027	0.013	8.31	18.31	0.04
SUS 316	0.06	0.74	1.75	0.026	0.006	12.91	17.39	2.48
SUS 310s	0.043	0.92	1.53	0.024	0.008	19.24	24.58	—

III. Results and Discussion

(III–1) Carbon Steel and Iron Single Crystal

Plastic deformation was induced by hydrogen charge in carbon steel and iron single crystal. The X-ray diffraction patters, taken from hydrogen charged specimens were

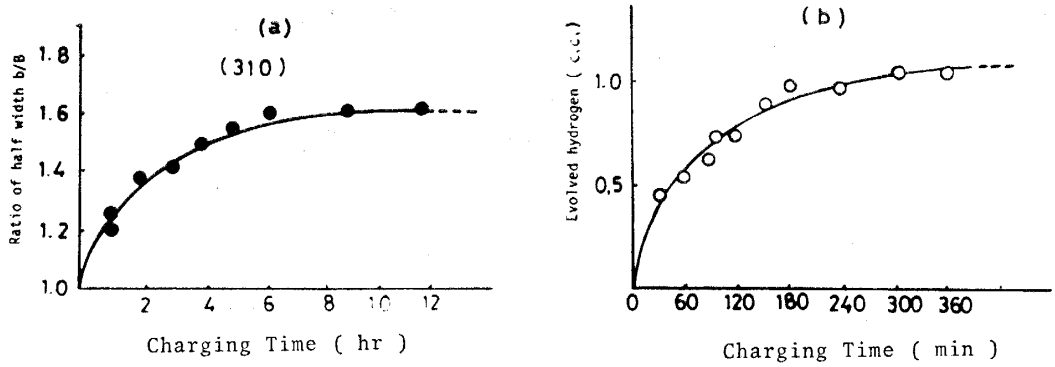

Fig. 1 (a) Change of half width ratio against hydrogen charging time.
(b) Evolved hydrogen after charging time. (At 45°C, 48 hr)

broadened. The half width of them are plotted against charging time in Fig. 1 (a). This plotts are compared with contented volume of hydrogen in Fig. 1 (b), which is measured from evolved gas when it was held in glycerin at 45°C for 48 hr.

An analysis of these broadened profiles was made by Tetelmann, Wagner and Robertson[7] using Warren-Averbacks[8] method which was re-examined by the author.

It was concluded that the diffraction line broadening caused from hydrogen charge consists of both sorts of broadening by lattice strain and by fragmentated small size of grain size. The broadness correspond to the one of 5% elongated specimen. For long time charging, the broadening by lattice strain saturates but the broadening by small particles size still increases. These hydrogen induced broadening of X-ray diffraction patterns did not recover at all, even if the hydrogen escaped from specimen by long time aging at room temperature. The recovery of it occured only by annealing at higher temperature than the recrystallization temperature, as shown in Fig. 2.

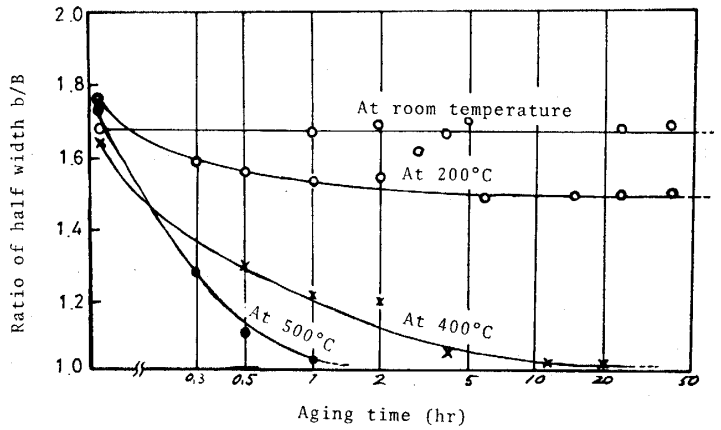

Fig. 2 Changing of half width with increasing time of aging.

Mechanical properties of tensile elongation and reduction of area were measured. They were reduced by hydrogen more and more with increasing the charging time, but the reduced ductility were recovered with increasing time of aging at room tem-

perature. Blisters or interior void, formed by hydrogen charge remainded but the mechanical properties were recovered at room temperature as shown in Fig. 3. From these facts, it can be considered that the main cause of hydrogen embrittlement is in the solid soluted hydrogen in the crystal lattice and the trapped hydrogen in voids play an auxiliary role on the embrittlement.

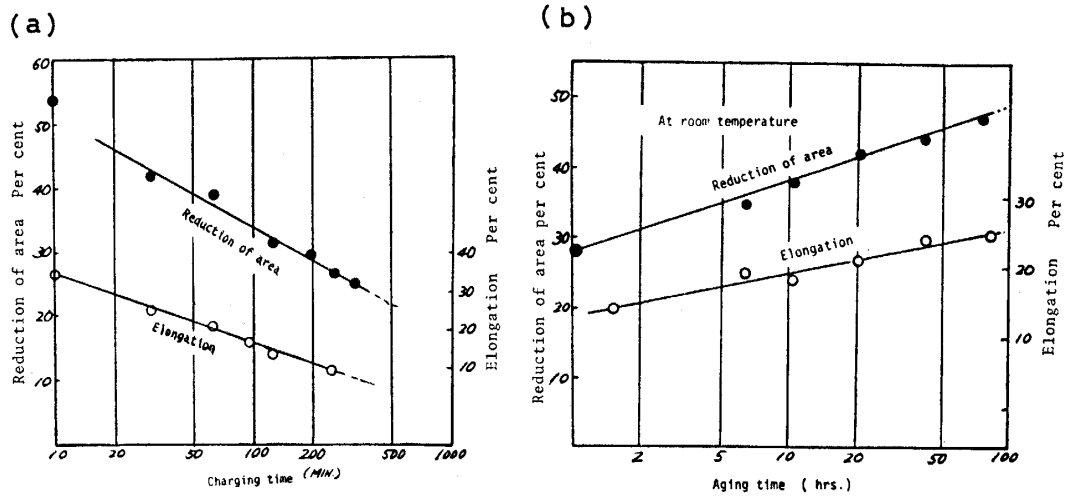

Fig. 3 (a) Reduction of ductility with the increasing time of hydrogen charge.
(b) Recovery of ductility with the increasing time of aging.

Detailed state of plastic deformation induced in crystals were examined using iron single crystal from the pseudo-Kossel patterns. A micro focus X-ray apparatus, having 20 micron focal size was used and back reflection pseudo-Kossel patterns were taken. The short exposure time of the method of no longer than 60 seconds enable us to observe the state of some instance without degassing.

These photographs of the pseudo-Kossel patterns are shown in Fig. 4. Photograph of Fig. 4 (a) is a initial state before hydrogen charge, which shows the crystal is nearly perfect, from its sharpness and smoothness of diffraction ellipsoid; (b) is a state after 6 min charge of hydrogen; (c) is after 10 min charge; and (d) is a photograph after 60 min hydrogen charge and aged for 100 hr at room temperature.

The diffraction ellipsoids of (b) and (c) are broadened. The broadening of the line increased with increasing time of hydrogen charge. The brokened blanks of the diffraction ellipsoids are incured by the lost of Bragg's condition owing to the blister formation or misorientation of crystalline blocks by hydrogen precipitation. They can be explain by the observation of topographic images taken from the specimen, using Berg-Barrett method, one of which is shown in Fig. 5.

In the Fig. 5, misboundaries are expressed by dotted line which appeared after hydrogen charge. Small blisters are formed at these small angle boundaries.

The discrepancies and local bend of the diffraction ellipsoid are caused from misorientation between adjacent crystalline blocks. Approximate estimation of disloca tion density is given using a simple model suggested by Hirsch[9] as shown in Fig. 6.

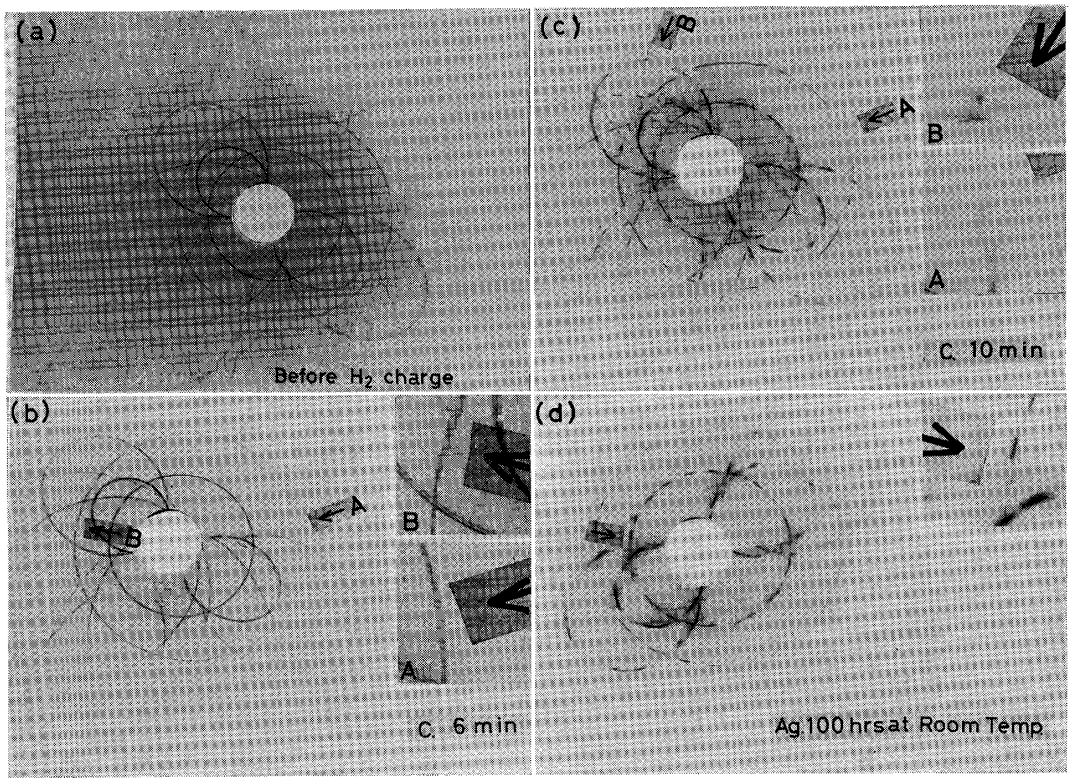

Fig. 4 Pseudo-Kossel patterns showing the plastic deformation by hydrogen charging and aging at room temperature.
(a) Initial state of hydrogen charge.
(b) 6 min hydrogen charge.
(c) 10 min hydrogen charge.
(d) 100 hr aging at room temperature after 60 min hydrogen charge.

The dislocation increased with the charging time of hydrogen, these aspect can be observed by transmission electron microscopy.

The depth of these distorted region is attained to about 400 micron thick after 60 minutes charge which was measured by the psudo-Kossel patterns taken from each eliminated surface little by little with electropolishing, untill the smooth and sharp ellipsoid is attained. These deformed layer dose not recovered to its original state, even if it is annealed at 750°C for 60 minuts.

The transmission Laue photographs of these hydrogenated single crystal are shown in Fig. 7. In this photograph, diffuse streak is followed on each Laue spots. This differs from asterism but resembled to the streak, which appear in the process of G. P. zone formation in Al–Cu alloy crystal.

Some coagulations of hydrogen, produced in a plate like is supposed from the patterns.

The thin plate like coagulations of dislocations were observed by transmission electron micrographs, but their diffraction patterns are quite obsque.

One of the most interesting point of the photograph is trippled spots of (310) reflection, but it is not yet fully analysed.

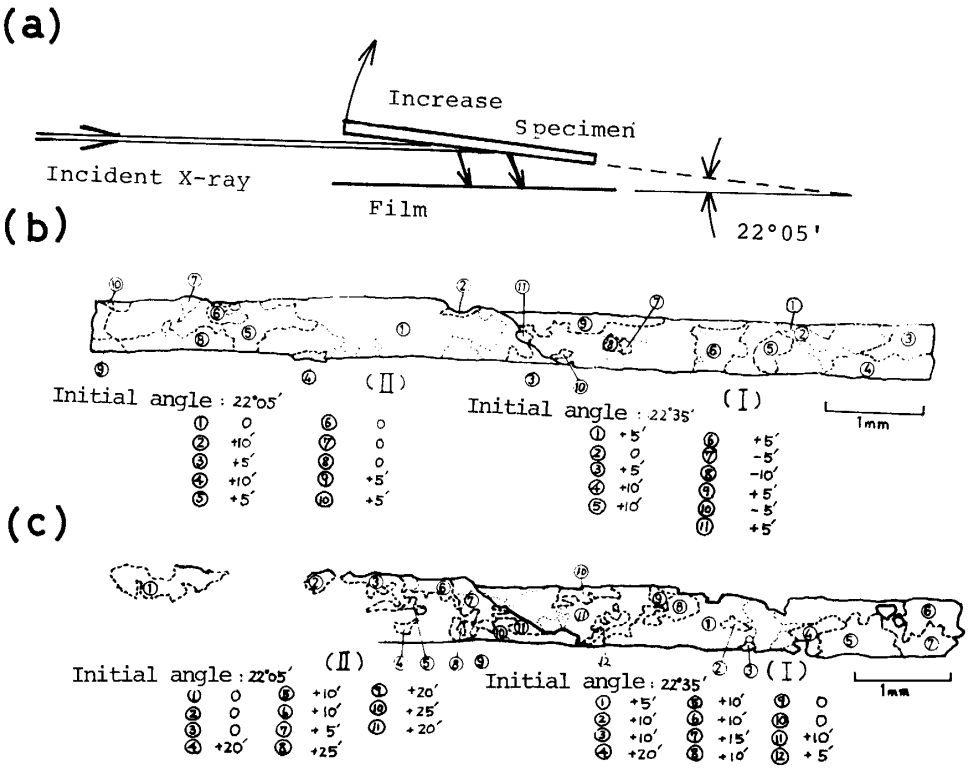

Fig. 5 Misorientation (dotted line) and blister, produced by hydrogen charge for 15 min.

(a) Schematic representation of Berg-Barrett method camera.
(b) Sketch of Berg-Barrett pattern before hydrogen charge.
(c) Sketch of Berg-Barrett pattern after 15 min hydrogen charge.

If hydrogen charged into wiska, it was difficult to reveal these streaks in its Laue photograph and also the streaks were promoted by slightly residued strain. From these facts, hydrogen should be trapped at misboundaries or other lattice defects and the streak should be caused from the irregularities of the crystal lattice in the order of the unit cell.

In the case of cathodic charging of hydrogen, it is introduced into metal as an ion. But from atmospheric environment, hydrogen must be adsorped on the metal surface and it permiate into metal by the energy change owing to the change of adsorption state from the s-state to the r-state or hydrogen is produced by galvanic action by the virture of wet corrosive surroundings.

To examine these state, pseudo-Kossel patterns were taken from specimens, which were held in high pressure hydrogen gas of 100~250 Kg/cm^2 at elevated temperature. Another specimens were immersed in dilute solution of HCl, H_2SO_4 and H_2S.

The diffraction lines of reflected ellipsoids show broadening and partly distorted, but the reaction was not so fast as cathodic charge. Fig. 8 is a result of the experiment after exposed to high pressure hydrogen gas at 250 Kg/cm^2.

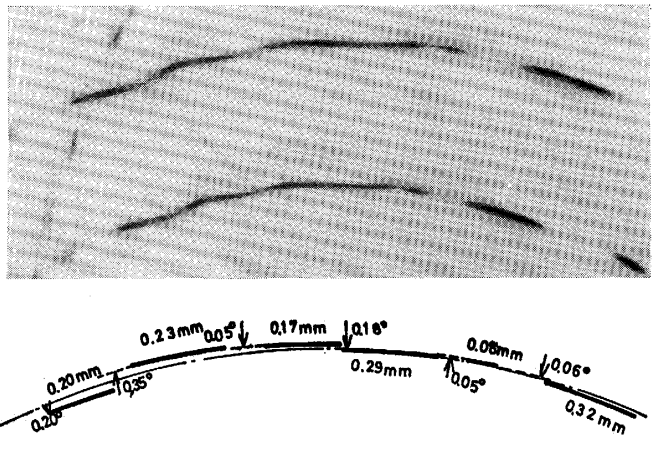

The widths and angles of shifts of the line on (211) pattern. (after 3 hr charge)

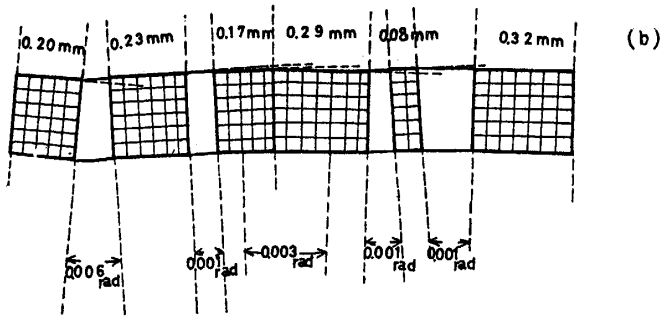

Fig. 6 Schematic representation of the misorientation of crystal lattice, which expressed as the bending and discrepancy of the pseudo-Kossel patterns, shown in (a).

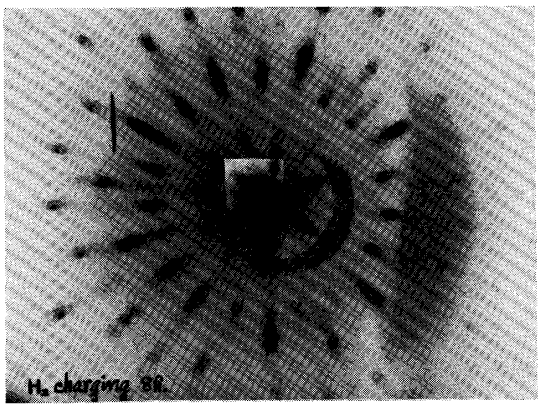

Fig. 7 Laue photograph, [110]// incident X-ray, diffuse streak is followed on each Laue spot.

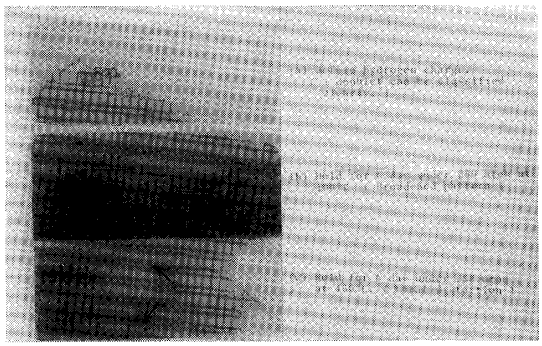

Fig. 8 Broadening and local distortion of pseudo-Kossel pattern by solid solute hydrogen, under high pressure at high temperature.

(III–2) Austenitic Stainless Steels

When hydrogen is charged into austenitic stainless steels various kinds of phase changes occurred such as hydride formation, phase transformation[10] of austenite to epsilon and alpha martensites and surface cracking[11].

Fig. 9 shows the X-ray diffraction patterns of SUS 304 steel, when it is hydrogen

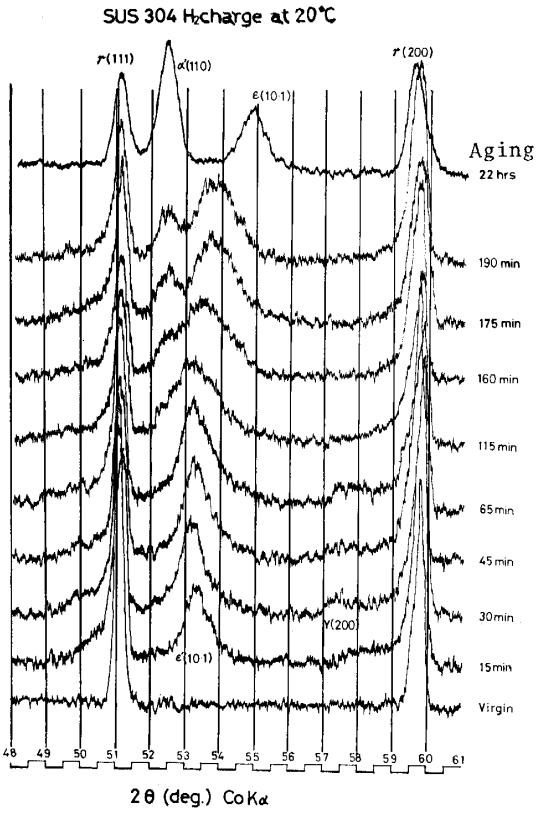

Fig. 9 X-ray diffraction patterns of SUS 304 charged at 20°C, showing variations of profiles with changing the hydrogen charging time.

charged by electrical method. At the early stage of hydrogen charge, f.c.c. hydride phase, designated "Y" from convenience, and a h.c.p. hydride ε' phases are formed. The (111) and (200) peaks of the Y phase are appeared at $2\theta=50°$ and $2\theta=57.5°$ respectively, when hydrogen is charged for 30 min. The lattice parameter of the Y and austenite γ are determinded to be $a=3.72$ A for Y and $a=3.589$ for γ. The peak intensity of the Y become prominent untill about 60 min charge, and at the same time, that of γ diminished progressively. (If the charging temperature is enrisen, the peaks of the Y revealed more prominent.)

After 160～180 min charge, the (110) peak of α' and (10·1) peak of ε are appeared, and the hydride phases of the Y and ε' are dimished of their intensity following with the growth of α' and ε. The appearance of intermediate phase ε' has not been reported in

another type of transformation process, it is a characteristic feature of hydrogen induced transformation. The peak of ε' shifts continuously to higher angle side with increasing time of hydrogen charge, and the (10·1) peak of ε' is separated completely into two peaks which are appeared at the angle of $2\theta=52.3°$ and 54°, that are correspond to (110) of α' and (10·1) of ε, respectively.

The ε' likely changes to ε continuously, but it is not so, and ε' is distinct from ε as shown in Fig. 10. The ε' phase is metastable at room temperature below 0°C, that is a lot of hydrogen absorved in ε lattice can not move at thus low temperature. Fig. 11 shows the X-ray diffraction profiles at low temperature from −78°C to room tem-

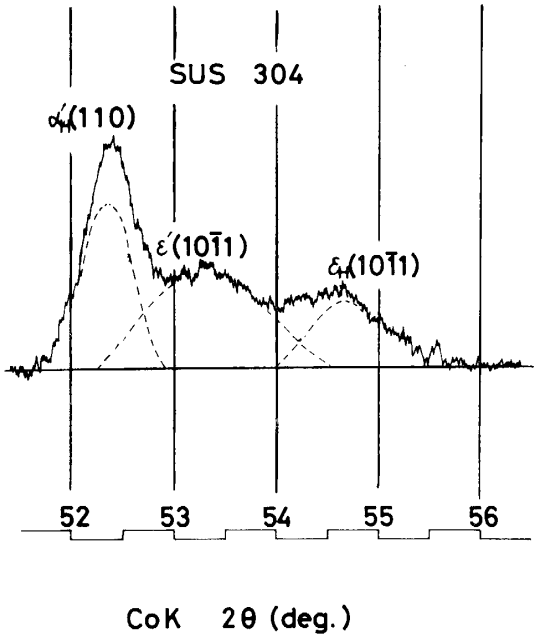

Fig. 10 A part of X-ray diffraction pattern showing the distinction among α', ε' and ε peaks.

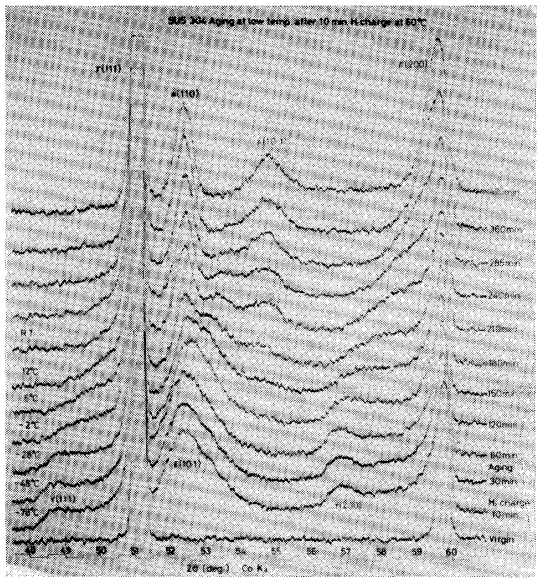

Fig. 11 Effect of aging time at increasing temperature gradualy from −78°C to room temperature after 10 min hydrogen charge at 60°C.

perature, from which it is clear that the transformation of ε' to ε and α' occurs at above 0°C. After long time aging at room temperature, the lattice parameter of α' and ε are determined to be $a=2.873$ for α' and $a=2.60$, $c=4.15$ and $c/a=1.60$ for ε respectively.

Fig. 12 shows the angular changes of X-ray diffraction peaks of various phases in SUS 304 type stainless steel with increasing the charging time. In order to compare those with the changes of lattice parameters of strain induced products with increasing strain amounts, strain percent is given at the top of the figure. The suffixes of H, W and Q mean hydrogen induced, strain induced and athermal products, respectively.

Comparing these three ways of producing martesite phases, it is to be noted that the (10·1) of ε_H peak position within 5 hr of the charging time, differs from (10·1) of ε_W and (10·1) of ε_Q peak positions. After aging, a hydrogen charged specimen at room temperature for a long time, its lattice parameters finally coinsides with those of ε_W

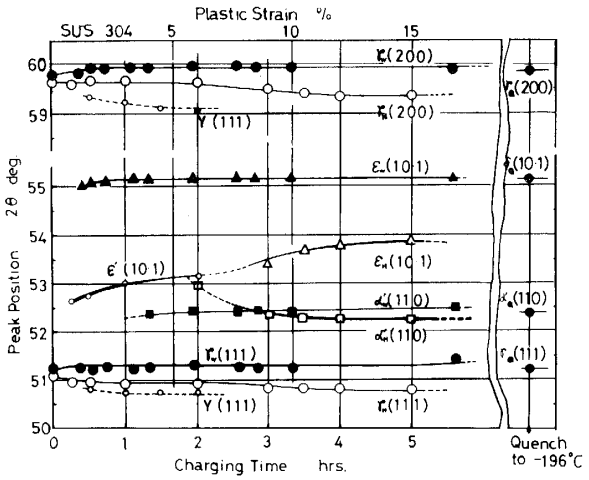

Fig. 12 Angular peak positions of X-ray line profiles of various phases, plotted on against charging time and plastic strain. Data for as-quenched sample are included. (SUS 304)

and ε_Q, because of releasing hydrogen in ε'.

From the above X-ray results, the sequence of the phase transformation in hydrogen induced phase transformation in SUS 304 is considered that: $\gamma \rightarrow Y + \varepsilon' \rightarrow \varepsilon + \alpha' \rightarrow \alpha'$.

It is to be noted that the transformed depth of hydrogen induced case has been limited in thin surface layer.

In the case of SUS 316 type stainless steel, Y and ε are formed by hydrogen charge but the α' is not so prominent as in SUS 304, meanwhile in SUS 310s type steel, only Y and ε' are formed. Both of Y and ε' transform reversibly to austenite by long time aging at room temperature, in these two sorts of steels.

The Y and ε' can be considered as phases of hydride, and not merely expanded lattice of γ or ε, from their distinct diffraction peaks, even though they are broadened. And these hydrides become more prominent with increasing contents of hydrogen that is increasing of Ni contents.

In the cases of higher Ni alloys than 30%, two sorts of Y_1 and Y_2 are formed as shown in Fig. 13.

These transformed phases were observed by transmission electron microscopy. Fig. 14 shows the transformation process. Fig. 14 (a) is a micrograph of a specimen

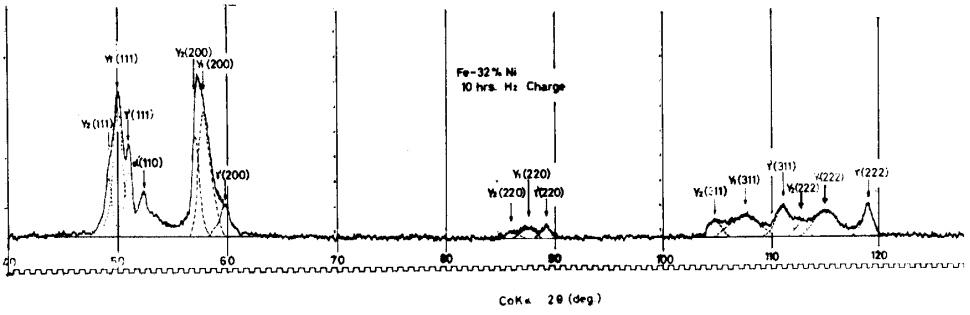

Fig. 13 (a)

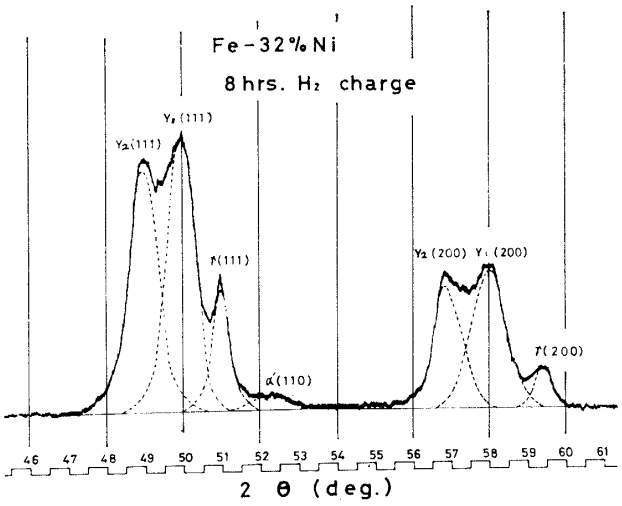

Fig. 13 (b)

Fig. 13 Hydrogen induced transformation. (Fe-32%Ni alloy)
(a) X-ray diffraction pattern after 10 hr hydrogen charge.
(b) X-ray diffraction pattern after 8 hr hydrogen charge.

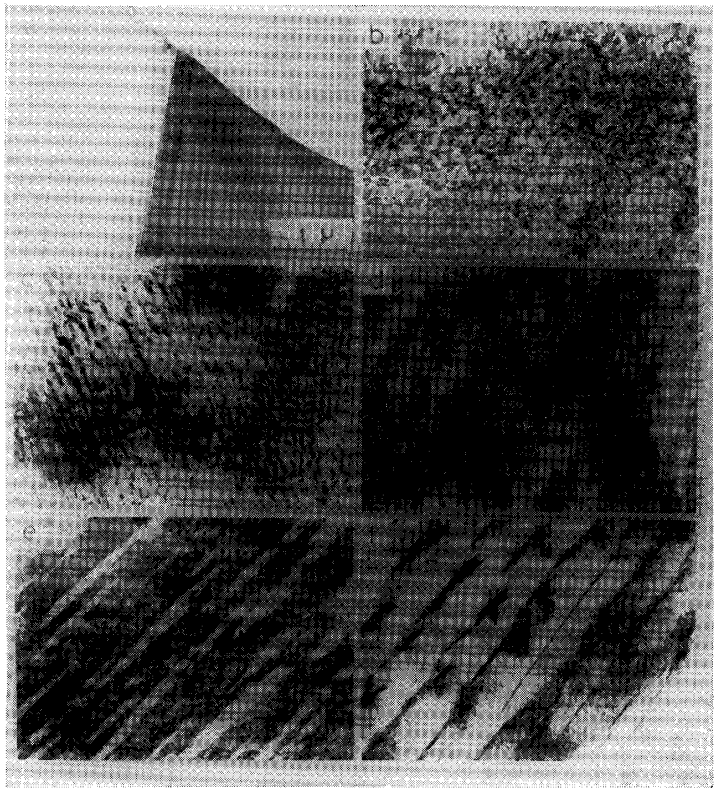

Fig. 14 Transmission electron micrographs showing the structure changes by hydrogen charging at room temperature.

quenched from 1050°C to room temperature. It shows clean austenite grains, which do not contain any transformation products except a few dislocations.

The following structural changes occured by hydrogen charge into austenite, as shown in Fig. 14 (b)~(f). A specimen charged 1 min exhibits dislocation lines and loops, as in (b), and a crystal structure is still austenite. (c) is 5 min charged, which involves much more dislocations and stacking faults. The formation of many stacking faults in austenite suggests that hydrogen lowers the stacking faults energy of austenite. Hydrogen charging expands the austenite lattice and causes the dislocation movement. However, austenite transform to ε' by 20 min. hydrogen charge which looks like rain cloud in (d). Since ε' is considered to be formed by absorping a lot of hydrogen, it involves many lattice defects and an electron microscopic structure is quite obscure. A specimen aged 3 hr after being charged 20 min reveal a composite structure of ε and α', as shown in (e). The dark band regions is ε and white bands are α'. The both phases were transformed from ε' as has been discussed in X-ray investigation. It is to be noted in this figure that α' lathes with the same variant have been formed. This fact will be leading the important result later. A specimen aged more than 24 hr after charged 20 min, almost transforms to α' lathes and retains a small amounts of ε which exist at the boundaries of α'-lathes as black and narrow bands in (f).

The electron diffraction pattern taken from the area including several α'-lathes, indicates consisting of only one zone axis. This means that α' bands transformed from ε which is seen in (e), grew to α' lathes in (f) during hydrogen charging and aging at room temperature. The sequence of the hydrogen induced transformations in 304 type steel can be proposed as follows; $\gamma \rightarrow Y + \varepsilon' \rightarrow \varepsilon + \alpha' \rightarrow \alpha'$.

A huge α' martensite was found in an 0.3 micron specimen charged 1 hr, as shown in Fig. 15. In this figure, the region of A and C were identified to be ε, and the white and broad band of B were α' of single crystal, which is 5 micron in width and 10 micron in length. This large size of α' were formed by merging of small α' lathes. Linear and

Fig. 15 Transmission electron micrograph of a hydrogen charged thin foil of SUS 304, showing a huge α' martensite in ε the phase.

black regions of ε remaind in B are considered to be remaind as a result of disappearing of α′ lath boundaries.

The dis-appearing of lath boundaries can be exprained that each of α′ lathes has the same orientation and lath boundaries easily migrate because of the thinness of a foil. Anywhere, such a large α′ martensite in austenitic stainless steels has not been reported so far.

Production of surface cracks by hydrogen charge has been reported, the density of the microcracks of SUS 304 and 316 type stainless steels are plotted in Fig. 16 against hydrogen charged time. These cracks grow continuously on the aging process at room temperature. If the specimen is stressed by repeated loading, these cracks are connected toward large macro crack.

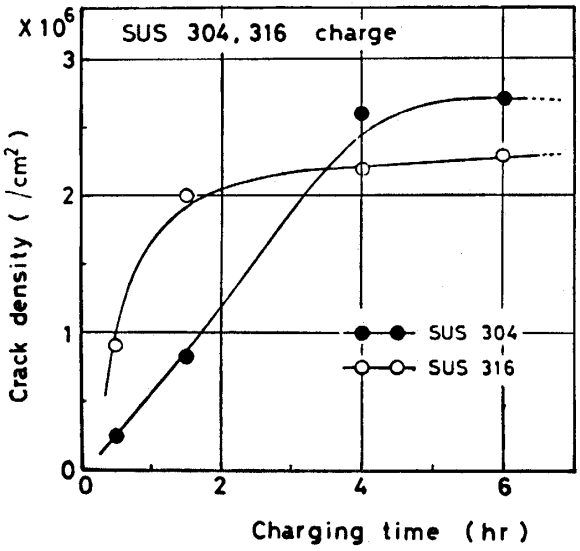

Fig. 16 Surface crack density of SUS 304, 316 are plotted against hydrogen charging time.

IV. Summary

When hydrogen is charged into carbon steel, the plastic deformation corresponding to 5% strained specimen by tensile test occures in the surface layer. Surface blisters and internal voids are also produced. Changes of the mechanical properties during hydrogen charging process and the following aging process show that the 1st cause of hydrogen embrittlement is solid soluted hydrogen and hydrogen in voids play a subsidiary role.

In the case of austenitic stainless steels, phase transformations are induced and it is closely related to hydride formation and decomposition, by cathodic charge of hydrogen. Another one of the effects of hydrogen charge is crack formation.

The *Y*, ε′, ε and α′ phases have been found as hydrogen induced products in SUS 304. The *Y* phase is an f.c.c. hydride and the ε′ is a metastable h.c.p. hydride. These two phases disappear in a certain time, following with phase transformation of ε and

α'. The ε' is an intermediate phase between γ and ε, which has larger lattice constant than that of ε, and transform to ε and α' after hydrogen charging and aging.

The ε and α' phases are crystallographically the same ones as are formed by cold working or cooling to temperature below Ms. But the transformation process and morphology in hydrogen charged steels are quite different from those in cold worked or quenched one. The transformation process in hydrogen charged stainless steels is as follows: $\gamma \rightarrow Y + \varepsilon' \rightarrow \varepsilon + \alpha' \rightarrow \alpha'$.

In higher Ni contented steels more than 30%, The Y and ε' are formed more prominent way than 304 steels, these hydride and their formation process should be described in recently.

References

1) Zapffe, C. A., Materials and Methods **32** (1953) 58.
2) Kazinczy, F., J. Iron Steel. Inst., **177** (1954) 85.
3) Petch, N. J., Nature, Lond. **169** (1952) 842.
4) Morlet, N. J., Johnson, H. H. and Troiano, A. R., J. Iron Steel. Inst., (1958) 37.
5) Plusquellec, J., Azou, P. and Bastien, P., C. R. Acad. Sci., Paris (1957) 1195.
6) E. Fujita, (Will be problished in near future.)
7) A. S. Telelmann, G. N. J. Wagner and W. D. Robertson. Acta Met., **9** (1961) 205.
8) Averbach, B. L. and B. E. Warren, J. Appl. Phys., **20** (1946) 1066.
9) P. B. Hirsh, "Progress in Metal Phys." Pergamon Press.
10) M. L. Holtzworth and M. R. Louthan, Corrosion **24** (1968), 110.
11) K. Kamachi and S. Miyata, Proc Mech Beh mat., J. S. M. S. vol.3 (1972) 274.